Sensors and Actuators Reports 5 (2023) 100146

Contents lists available at ScienceDirect

Sensors and Actuators Reports

journal homepage: www.sciencedirect.com/journal/sensors-and-actuators-reports

Stable hemoglobin-based biosensor based on coordination-assisted microfluidic technology for hydrogen peroxide determination

Rongwei Gao, Yiqi Song, Yuan Gao, Xuelian Yang, Shu-Juan Bao *

Key Laboratory of Luminescence Analysis and Molecular Sensing, Ministry of Education, School of Materials and Energy, Southwest University, Chongqing 400715, PR China

ARTICLE INFO

Keywords:
Hemoglobin-based biosensor
Coordination assisted
Microfluidic technology
Hydrophobic ionic liquid (HIL)
Microenvironment

ABSTRACT

Enhancing the stability and sensitivity of electrochemical biosensors is highly significant for their practical application. Herein, inspired by the formation of mussel foot protein, we proposed a strategy to construct a hemoglobin-based biosensor for hydrogen peroxide detection using a hydrophobic ionic liquid (HIL) coordination assisted microfluidic technology. The active layer HIL@Hb was achieved by mixing $BBimPF_6$ (HIL) and Hb via a microfluidic channel, in which HIL helps to maintain the conformational dynamic mobility of hemoglobin (Hb), while the coordination process in a microfluidic reactor prevents aggregation of Hb. Further, the electrode surface was modified with ultra-thin MXene-Ti_3C_2 nanosheets to ensure the effective adhesion of active layer and collection of sensing signals, thus improving the sensitivity of the sensor by synergistic catalysis. Experimental results demonstrate that our designed sensor has good repeatability and stability, which can retain 93% of the initial current response after 30 uses and about 90.11% of its primary current response to H_2O_2 after 30 days. And it has a good linear response range of 1.996–27.232 μM, detection limit reaching 1.996 nM (signal-to-noise ratio, $S/N = 3$), sensitivity of 52.08 $\mu A \cdot \mu M^{-1} \cdot cm^{-2}$. Overall, this research offers a facile and effective strategy for constructing a stable biosensor to effectively detect hydrogen peroxide.

1. Introduction

Hemoglobin (Hb), a special redox protein, has received widespread attention because of its good selectivity to hydrogen peroxide, thus, has been employed in numerous sensing technologies[1,2]. However, because Hb is easily inactivated after being separated from the biological environment, tremendous efforts have been devoted to enhance its stability and application potential[3,4]. In recent years, a large number of bioconjugation strategies have been developed to immobilize Hb, such as using (bio-) polymers[5,6], metal organic framework materials to encapsulate hemoglobin[7–9], sol-gel methods[10,11], porous materials to adsorb Hb[12–14], etc. Nevertheless, the factors affecting Hb activity are not only related to the strength of the interaction force between the immobilized carrier and hemoglobin, but are also affected by the immobilized microenvironment. Generally, the bio-friendly microenvironment for preparing an enzyme-based biosensor should: (i) maintain high intrinsic activity; (ii) limit exposure time to environmental stress; and (iii) not hinder the conformational dynamic mobility of the enzyme. While most traditional methods can improve the stability of Hb and enhance catalytic activity[15–17], only a few can maintain the conformational dynamic mobility of immobilized Hb.

In addition, hemoglobin is generally "inactive" and exhibits a closed form in aqueous media due to its active sites covered by hydrophobic amino acid chains[18,19]. And the electroactive centers of Hb are deeply buried in its hydrophobic cavity, delaying electron transfer and subsequently limiting the practical application of hemoglobin sensors [20,21]. HIL is composed entirely of anions and cations and takes on liquid form at or near room temperature, also showing good solubility, absorption, and stability[22,23]. Interestingly, HIL can act as a "two--handed weapon." On one hand, the imidazole cation of HIL coordinates with the ferrous ion of Hb, realizing the effective immobilization of Hb [24–26]. The combination of HIL and hemoglobin driven by hydrophobic and electrostatic interaction, which helps the expansion of the temporal polypeptide of Hb and ensures the dynamic migration of its conformation[27]. On the other hand, the hydrophobic surface of HIL helps to "open" Hb, thereby exposing its active center – a process called "interfacial activation" and enhancing its biocatalytic activity[28]. However, because of the strong trapping power of HIL, Hb can easily aggregate in HIL, which greatly decreases its biocatalytic activity.

Inspired by the behavior of mussels, we came up with the idea of

* Corresponding author.
E-mail address: baoshj@swu.edu.cn (S.-J. Bao).

https://doi.org/10.1016/j.snr.2023.100146
Received 1 September 2022; Received in revised form 9 December 2022; Accepted 28 February 2023
Available online 11 March 2023

using coordination assisted microfluidic technology to inhibit the aggregation of Hb and enhance the repeatability and stability of enzyme biosensor. It is reported that the shellfish first absorb iron and vanadium ions from seawater and store them in metal storage sacs compounded with catechol molecules in the cells[28]. The mussel foot protein is secreted by the shellfish, the concentrated protein solution and the metal were stored respectively. The two types of secretion capsules of ions are mixed in the microfluidic channel-like duct network and form protein-metal bonds in the newly formed bypass[29,30]. Metal coordination provides strong adhesion and enhances the mechanical stability of silk protein. Herein, we used a microfluidic channel as a microreactor to immobilize Hb in HIL and construct an active layer of HIL@Hb, which can effectively prevent the aggregation of Hb. As shown in Scheme 1, more wrinkles formed on the surface of the electrode surface synthesized using the microfluidic channel, subsequently enhancing the effective sensing area for more target molecules. Moreover, to obtain a sensitive biosensor, the effective collection and rapid transfer of electrons between Hb and the electrode is also highly important. Thus, ultra-thin MXene-Ti_3C_2 nanosheets were introduced to modify the electrode surface[31–33]. The rough 2D structure of MXene-Ti_3C_2 is conducive to adhere HIL@Hb on the electrode surface; while the excellent conductivity of MXene-Ti_3C_2 can effectively reduce contact resistance and support fast electron transfer. Interestingly, the good selective sensing of MXene-Ti_3C_2 to H_2O_2 can improve the sensitivity of the sensor by synergistic catalysis[34]. Overall, this work proposes an effective strategy to construct a stable and sensitive enzyme sensing platform, which is promising for enhancing the sensor's stability and sensitivity.

2. Experimental

All chemicals and apparatus are given in the Supporting Information.

2.1. Fabrication of MXene-Ti_3C_2 nanosheets

The ultra-thin MXene-Ti_3C_2 nanosheets (1.0 mg mL^{-1}) were prepared following our previously reported method[4,35].

2.2. Bulk solution synthesis of HIL@Hb

The Hb solution was prepared by dispersing 0.1 mg Hb in 1 mL phosphate buffer solvent (PBS, pH = 7.24) at room temperature. 1.6 mL $BBimPF_6$ ionic liquid, as the HIL, and Hb solution were mixed with good shaking, then the mixture was left alone for 10 min. After the liquid stratified, the supernatant was removed, and the solution was stored in a refrigerator at 4 °C.

2.3. Microfluidic flow synthesis of HIL@Hb active layer

$BBimPF_6$ ionic liquid and Hb solution (100 μg mL^{-1}) were introduced into different inlets of a microfluidic chip (74,900 Cole-Parmer, USA) by a syringe pump at room temperature. The flow rate of $BBimPF_6$ was 80 μL min^{-1}, and the injection speed of Hb solution was 50 μL min^{-1}. After 3 min, the product was collected from the outlet and used as the active layer.

2.4. Preparation of HIL@Hb/MXene-Ti_3C_2/SPCE

As shown in Scheme 2, screen-printed carbon electrodes (SPCE) were prepared by forming the working and counter electrodes with carbon paste and the reference electrode with Ag paste, following our previously reported method. Next, the reaction cell was prepared by stably fixing part of a 1 mL pipette tip (5-mm deep) on the end of SPCE to perform cellular inoculation[36].

Subsequently, 2.5 μL ultra-thin MXene-Ti_3C_2 nanosheet solution (1.0 mg mL^{-1}) was dropped onto the surface of SPCE for modification. Then, the HIL@Hb active layer was dropped onto the surface of the modified electrode and dried at room temperature. Before in situ cell cultivation, the HIL@Hb/MXene-Ti_3C_2/SPCE was sterilized with UV irradiation for 30 min, followed by inoculation of 4T1 cells (1×10^5 mL^{-1}) in the prepared reaction cells. After the cells were cultured for 9 h get the obtained 3D in situ fixed cells electrode and further used them for electrochemical sensing to H_2O_2.

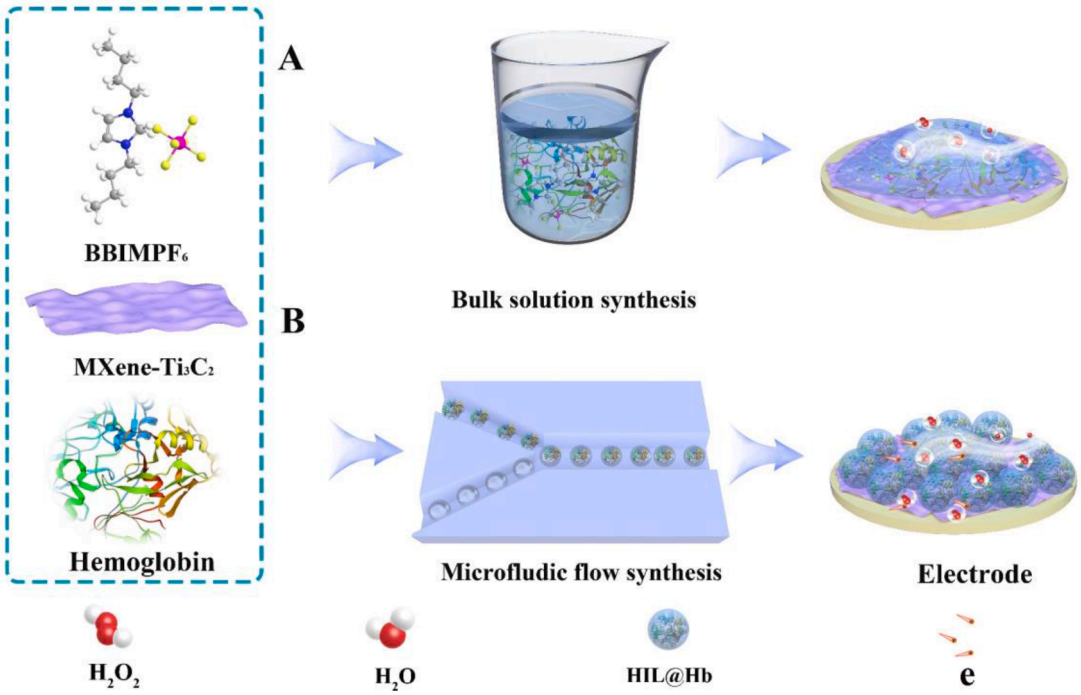

Scheme 1. Schematics of different mixing methods of Hb and HIL in (A) bulk solution and (B) microfluidic laminar flow.

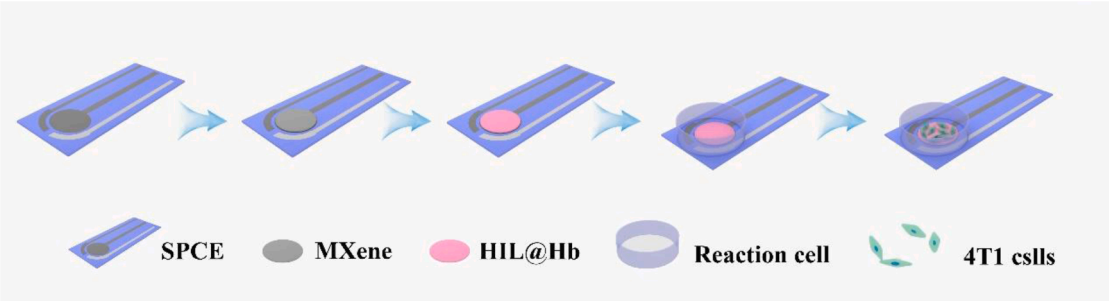

Scheme 2. Preparation of HIL@Hb/MXene-Ti_3C_2/SPCE.

3. Results and discussion

3.1. Selective extraction of Hb in $BBimPF_6$

Herein, $BBimPF_6$ was used as the HIL to extract hemoglobin from the aqueous hemoglobin solution. As shown in Fig. 1a, the aqueous phase of the HIL@Hb bulk solution before extraction was turbid due to the presence of a high concentration of Hb. while the Hb after extraction was almost transferred to the hydrophobic ionic liquid phase, and becoming a clear and transparent water phase. It has been reported that the high effective extraction of Hb by HIL is mainly driven by the imidazole cationic fragment of HIL, which interacts with hydrophobic residues in the substructure region of Hb[26]. Specifically, HIL can help the hemoglobin polypeptide to unfold, causing the contact angle to decrease (see Table S1). The fluorescence spectra in Fig. 1b shows the effect of HIL on different concentrations of Hb under an excitation wavelength of 365 nm, where HIL is displayed blue. With increasing Hb concentration, the fluorescence of the $BBimPF_6$ gradually weakened, and finally the fluorescence is quenched, which is consistent with the fluorescence spectrum (Fig. 1c).

Fig. 1c shows the fluorescence spectra before and after Hb extraction by $BBimPF_6$ (from top to bottom, the concentration of Hb gradually increases). When an excitation wavelength of 365 nm was used, an obvious emission at 445 nm was observed, which is attributed to the π–π^* conjugate of N–C–N bonds in $BBimPF_6$. With increasing Hb concentration, the emission peak intensity of $BBimPF_6$ gradually weakened and red shifted from 445 nm to 500 nm, indicating the complete extraction of Hb by HIL. Further, the enzyme activity was studied by UV-Visible spectroscopy. It has been reported that Hb has an absorption peak at 410 nm. As shown in Fig. 1d, as the Hb concentration increased at 410 nm, the intensity of $BBimPF_6$ also increased ($R^2 = 0.997$). Which calculated by using the reported method, the extraction efficiency of

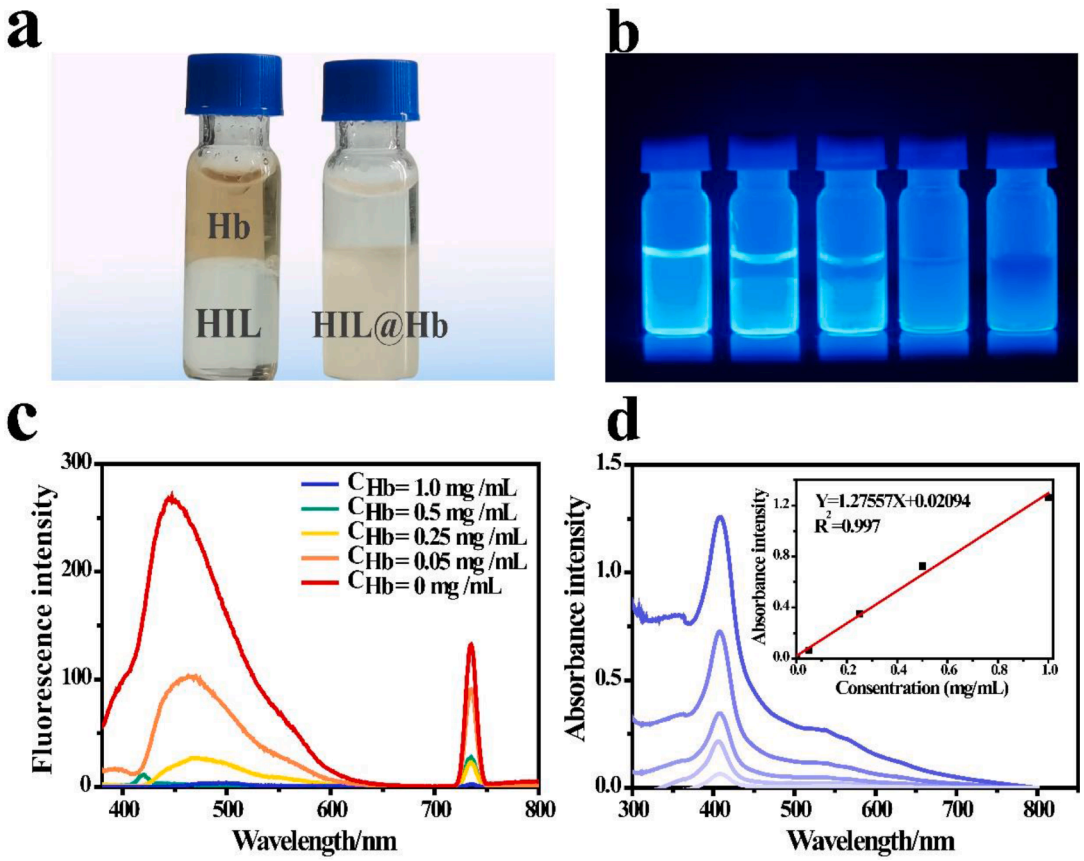

Fig. 1. a) Comparison photograph before and after Hb extraction with $BBimPF_6$. b) Sterilization of increasing concentrations of Hb (left to right) mixed with $BBsimPF_6$ under UV irradiation. c) Fluorescence spectra of increasing concentrations of Hb mixed with $BBimPF_6$ under an excitation wavelength of 365 nm. d) UV–Vis spectra of after extracted Hb with $BBimPF_6$ for 10 min (from top to bottom, the concentration gradually increases).

$BBimPF_6$ to Hb is 97.3% in our work[25]. And the peak position of Hb has not shifted, indicated Hb retained natural activity after extraction by HIL.

3.2. Structural features of HIL@Hb/MXene-Ti_3C_2

The total activity of Hb immobilized by bulk synthesis and microfluidic synthesis methods was evaluated by a reported method[37], as shown in **Fig. S1,** and the results are listed in Table S2. The total activity of Hb immobilized in the microfluid was 16% greater than that immobilized in the bulk solution, which indicates the effectiveness of the microfluidic reactor to inhibit Hb aggregation.

The morphology of HIL@Hb/MXene-Ti_3C_2 was also observed by field-emission scanning electron microscopy (FESEM). As shown in Fig. 2, good HIL@Hb film was formed with both methods due to the good film-forming properties of $BBimPF_6$ and a strong interaction with Hb[38,39]. As expected, the HIL@Hb/MXene-Ti_3C_2 electrode prepared by bulk solution synthesis (HIL@Hb/MXene-Ti_3C_2/BGCE, Fig. 2a) exhibited a large number of HB molecules completely wrapped by the HIL. Comparatively, due to a low Reynolds number of the flow inside the microchannel, the HIL@Hb/MXene-Ti_3C_2 electrode prepared using the microfluidic reactor (HIL@Hb/MXene-Ti_3C_2/MGCE, Fig. 2c) presented a laminar flow phenomenon, which is very similar to the formation of the mussel foot protein[40]. The two types of secretory capsules containing concentrated protein stock solution and metal ions are mixed in the microfluidic channel-like duct network, and protein-metal bonds are formed in the new bypass. One after another tiny vesicles are mixed through the microfluidic channel, and the coordination of the hydrophobic ionic liquid provides a strong adhesion force, which draws these vesicles closer to the stack, thus forming more wrinkled structures. This can enlarge surface-to-volume ratio and shortened diffusion distance of Hb in HIL. While the thickness of the two electrodes was almost same (Fig. 2b and d), the HIL@Hb/MXene-Ti_3C_2/MGCE surface was rougher, which is also consistent with the above results. In summary, by imitating the formation of mussel foot protein using a microfluidic reactor can maintain the activity of Hb and effectively increase the substrate contact area, reducing the substrate diffusion distance through the adjustment of the mixing process parameters.

3.3. Electrochemical measurements

The electrochemical activity of HIL@Hb/MXene-Ti_3C_2 sensing electrode was first evaluated by cyclic voltammetry (CV) in PBS (0.01 M, pH 7.24) at 50 mV s^{-1}. As shown in Fig. 3a, the HIL@Hb/MXene-Ti_3C_2/BGCE electrode exhibited a pair of un-conspicuous and asymmetry redox peaks at −92 mV and −211 mV. The difference in peak potentials (ΔE_P) of about 121 mV suggests that the direct electron transfer (DET) rate of Hb and GCE is extraordinarily slow, and merely few electroactive centers of Hb can exchange electrons[41]. This can be attributed to the fast synthesis of the bulk solution that causes Hb to embed inside and realize DET. However, compared with HIL@Hb/MXene-Ti_3C_2/BGCE, HIL@Hb/MXene-Ti_3C_2/MGCE showed a pair of clearly visible and symmetrical redox peaks at −175 mV and −243 mV, corresponding to the heme Fe (III/II) redox peaks of hemoglobin. The ΔE_P value was determined to be 68 mV, which is 53 mV less than that of HIL@Hb/MXene-Ti_3C_2/BGCE. This value also indicates a quasi-reversible and fast electron transfer characteristic, suggesting that DET of Hb was achieved on the electrode surface. Overall, these findings reveal that microfluidic mixing is more effective to construct a highly sensitive electrode surface.

The change in anodic (i_{pa}) and cathodic (i_{pc}) peak currents of HIL@Hb/MXene-Ti_3C_2/MGCE with increased scan rate was measured. Fig. 3b and 3c display a good linear relationship between the peak currents, which indicates that the reaction on the HIL@Hb/MXene-Ti_3C_2/MGCE is a well surface-controlled process. This result further confirms that our proposed HIL@Hb/MXene-Ti_3C_2/MGCE electrode is a promising electrochemical sensor.

The applicability of the different electrodes for detecting H_2O_2 was studied using CV in 0.01 M PBS with a pH of 7.4. As shown in Fig. 4, an obvious polarization phenomenon was observed for the bare electrode (Fig. 4a). After the electrode was modified with ultra-thin MXene-Ti_3C_2 nanosheets, the polarization phenomenon disappeared, and a perfect rectangle CV curve achieved due to the super conductivity of MXene-Ti_3C_2 (Fig. 4c). In addition, both HIL@Hb/GCE and HIL@Hb/MXene-Ti_3C_2/MGCE exhibited redox peaks (Fig. 4b and d), which are attributed to the electrochemical conversion between Fe (II) and Fe (III) of Hb. However, the redox peak of HIL@Hb/MXene-Ti_3C_2/MGCE is more obvious and symmetrical, whereby the electrical conductivity of MXene-Ti_3C_2 can enhance the electron transport performance. Using 0.0196 μM H_2O_2 solution, an obvious current response was observed for MXene-Ti_3C_2/GCE electrode, which suggested MXene-Ti_3C_2 could accelerate the reduction of hydrogen peroxide. Of course, as expected a more obvious current response appeared for HIL@Hb/MXene-Ti_3C_2/MGCE electrode which from the contribution of Hb and MXene-Ti_3C_2.

Considering that selectivity is a very important indicator for evaluating the feasibility of a biosensor, an anti-interference experiment was carried out. As displayed in **Fig. S3**, MXene-Ti_3C_2 demonstrated a strong catalytic performance for H_2O_2 and excellent selectivity for electrochemical sensing of H_2O_2. The electrochemical catalytic ability of MXene-Ti_3C_2 toward hydrogen peroxide was further confirmed by UV–vis and electron paramagnetic resonance (EPR) spectroscopy. The resulting spectra showed that MXene-Ti_3C_2 can completely reduce H_2O_2 to H_2O (**Fig. S4**). Thus, compared with the HIL@Hb/GCE, HIL@Hb/MXene-Ti_3C_2/MGCE has a greater electrocatalytic ability to reduce H_2O_2 and selectivity for H_2O_2. This better performance can be owed to MXene-Ti_3C_2, which supports the synergistic catalysis of H_2O_2, signal amplification, and improved sensitivity of the sensor. Meanwhile, excellent conductivity and small specific surface area can enhance electron transmission and collection efficiency.

In practice, the stability and sensitivity of biosensor are particularly important. Fig. 5a shows that a quick and continuous stepwise current response appeared at −0.35 V by successively adding H_2O_2 into an N_2-saturated 0.01 mol L^{-1} PBS solution. The calibration plots between H_2O_2 concentration and sensing current are displayed in Fig. 5b. A good linear response range of 1.996–27.232 μM, detection limit reaching 1.996 nM (signal-to-noise ratio, $S/N = 3$), sensitivity of 52.08 $\mu A \cdot \mu M^{-1} \cdot cm^{-2}$, and fast response time of 3.0 s were achieved (Fig. 5c). Furthermore, the reported hemoglobin-based H_2O_2 sensors and their sensitivity, detection

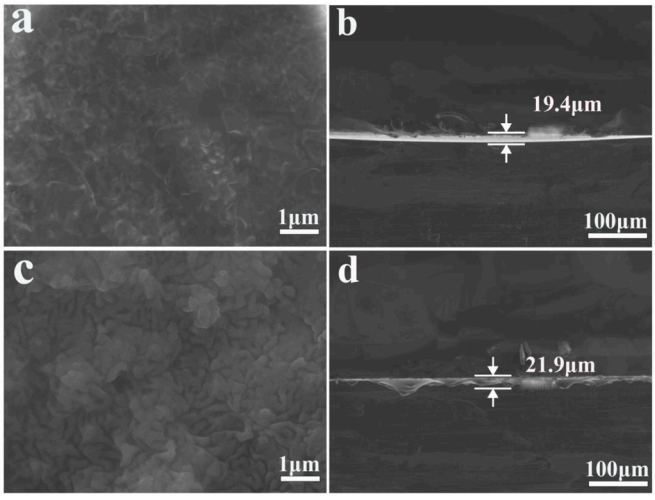

Fig. 2. a) FESEM image of HIL@Hb/MXene-Ti_3C_2/BGCE. b) Middle cross-sectional FESEM image of HIL@Hb/MXene-Ti_3C_2/BGCE. c) FESEM image of HIL@Hb/MXene-Ti_3C_2/MGCE. d) Middle cross-sectional FESEM image of HIL@Hb/MXene-Ti_3C_2/MGCE.

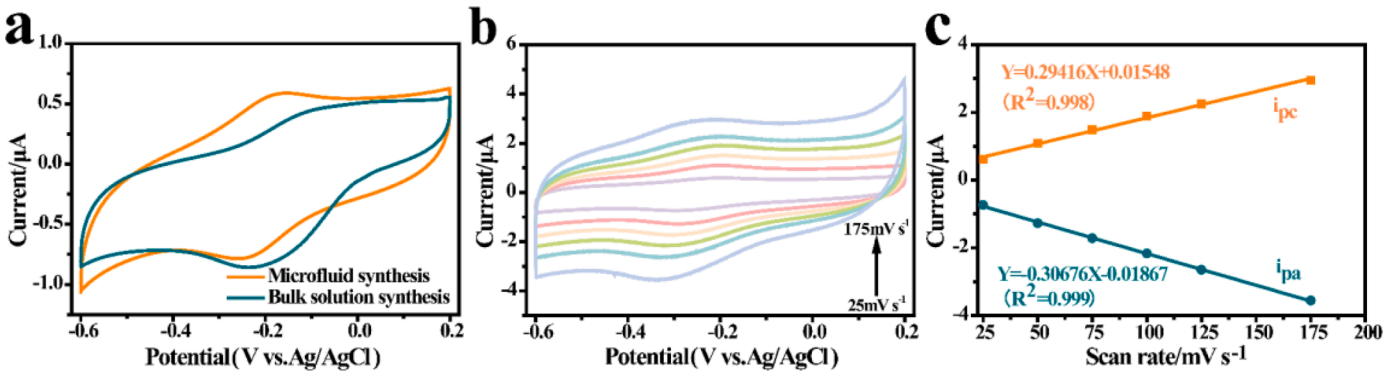

Fig. 3. a) CV curves of different modified GCE in 0.01 mol L^{-1} N_2-saturated PBS at 50 mV s^{-1}. b) CV curves recorded at HIL@Hb/MXene-Ti_3C_2/MGCE in 0.01 mol L^{-1} PBS at different scan rates (from 25 to 175 mV s^{-1}, inside to outside). c) Plots of peak currents versus scan rate.

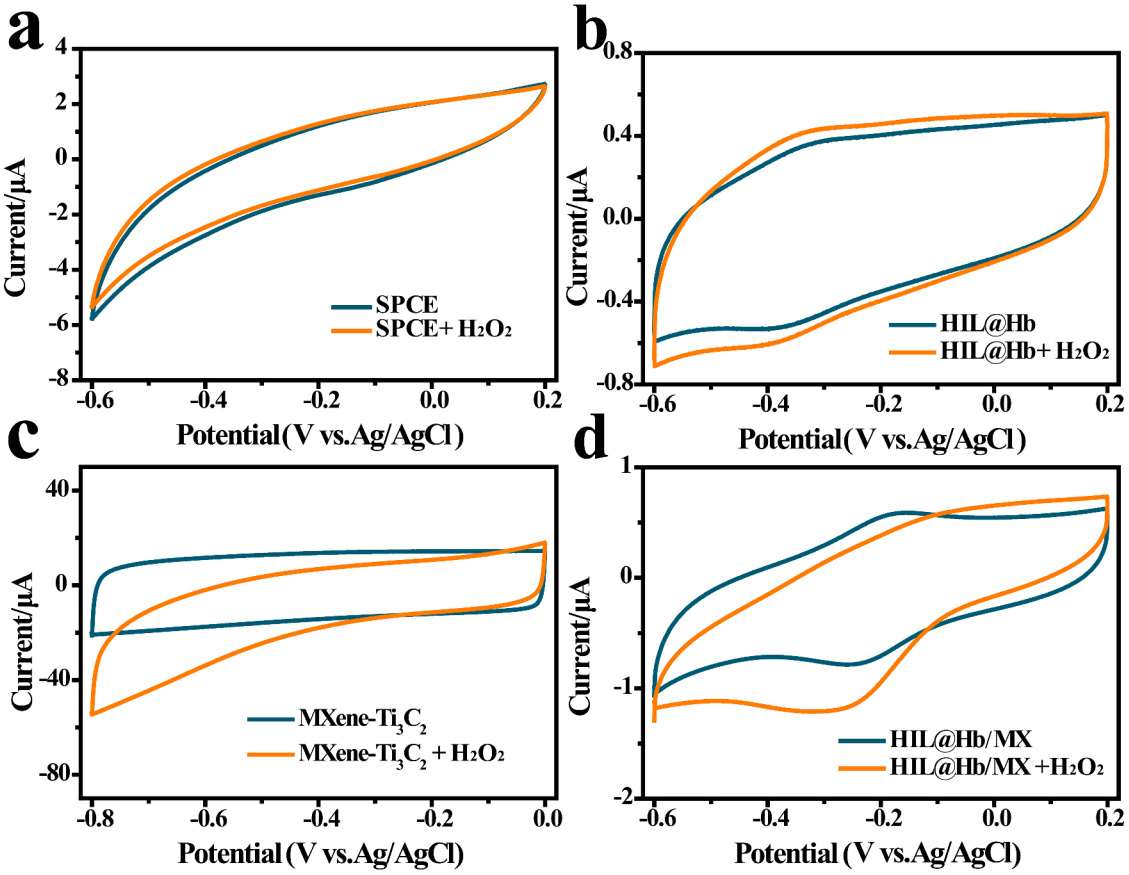

Fig. 4. CV of the response to H_2O_2 recorded at different modified GCE in 0.01 mol L^{-1} N_2-saturated PBS at 50 mV S^{-1}. a) SPCE; b) HIL@Hb/GCE; c) MXene-Ti_3C_2/GCE; d) HIL@Hb/MXene-Ti_3C_2/MGCE.

limit, and detection range are listed in **Table S3**, among of these results, the HIL@Hb/MXene-Ti_3C_2/MGCE sensor shows the highest sensitivity, lower detection limit and good linear range. In addition, the Apparent Michaelis-Menten constant (k_M^{app}) can be used to predict the enzyme-substrate kinetics. As we all know that the smaller value of k_M^{app} suggested the enzyme activity is higher and affinity toward the substrate is better, and the constant k_M^{app} can be gained from the electrochemical-version of the Lineweaver–Burk equation[42,43]:

$$\frac{1}{i_{ss}} = \frac{k_M^{app}}{i_{max}} \frac{1}{c} + \frac{1}{i_{max}} \quad (1)$$

where i_{ss} is the steady-state current after substrate addition; i_{max} is the maximum current tested under saturated substrate conditions; and c refers to the H_2O_2 concentration. Using Eq. (2), k_M^{app} of HIL@Hb/MXene-Ti_3C_2/MGCE was calculated to be 2.24 μM, which is smaller than 16.86 μM of HIL@Hb/MXene-Ti_3C_2/BGCE, suggesting that Hb immobilized on HIL@Hb/MXene-Ti_3C_2/MGCE can maintain a higher enzyme activity, and also represent it has a greater biological affinity and catalytic performance to H_2O_2. Therefore, the plot of amperometric response versus the detected H_2O_2 concentration illustrates a well-defined and typical behavior of an enzymatic kinetic reaction. Further, compared with HIL@Hb/MXene-Ti_3C_2/BGCE (**Fig. S5**), the current response of HIL@Hb/MXene-Ti_3C_2/MGCE showed to be stronger and more stable. Comparatively, HIL@Hb/MXene-Ti_3C_2/BGCE exhibited a fluctuating i-t curve, low sensitivity, and narrow response range. Several reasons for

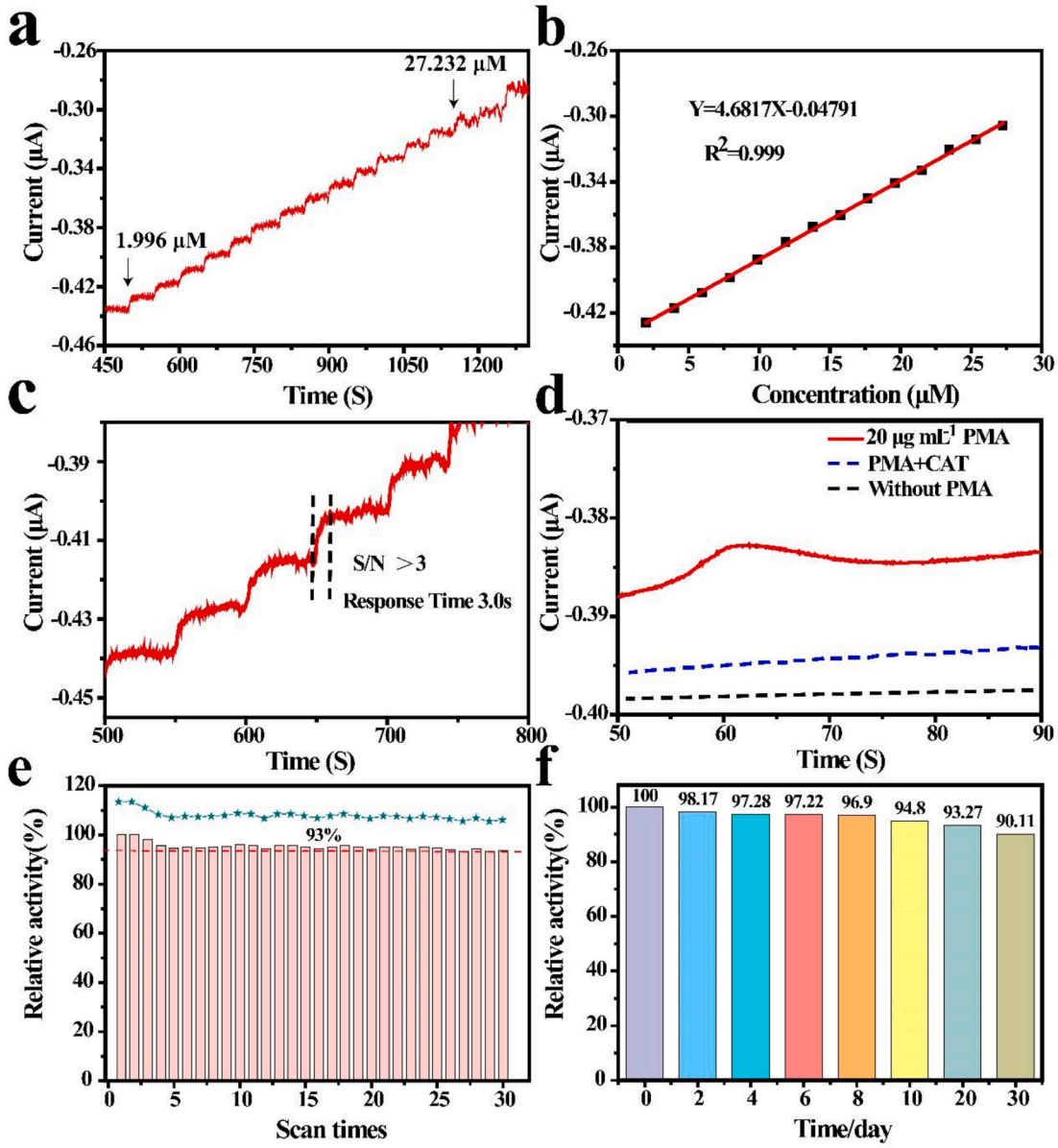

Fig. 5. a) Typical amperometric i-t curve for successive addition of different H_2O_2 concentrations of the sensor at −0.35 V. b) The linearly relationship between current and H_2O_2 concentration. c) Response time of the sensor. d) Electrochemical response of HIL@Hb/MXene-Ti_3C_2/MGCE toward H_2O_2 released by suspension of 4T1 cells. e) The stability of HIL@Hb/MXene-Ti_3C_2/MGCE chip continuously tested 30 times. f) Thirty-day stability of assembled HIL@Hb/MXene-Ti_3C_2/MGCE chip.

the better performance of HIL@Hb/MXene-Ti_3C_2/MGCE are subsequently described. Firstly, the unique and rich ridge-like fold structure of the microfluidic reactor enhances the contact area for detecting the target molecules. And in which, hydrophobic ionic liquid can help Hb gradually unfolds, the distance of electron transfer was shortened, and the electroactive center was exposed, so accelerates the speed of electron transfer. Secondly, ultra-thin MXene-Ti_3C_2 nanosheets were introduced to modify the electrode surface, greatly increasing the effective area and enhancing the stability of the electrode interface. Moreover, MXene-Ti_3C_2 promotes the electron transport efficiency, thereby obtaining an amplified electrochemical response signal. Thirdly, the synergistic catalysis of enzyme and non-enzyme enhances the sensitivity and catalytic efficiency of the biosensor. In general, because of these advantages of HIL@Hb/MXene-Ti_3C_2/MGCE that it has rapid response to H_2O_2 and outstanding linear range, so the HIL@Hb/MXene-Ti_3C_2/MGCE is used for further research in determination of H_2O_2 released by cells.

3.4. In situ detection of hydrogen peroxide released from living cells

H_2O_2 is closely correlated with signal transduction and cell fate decisions, this sensitively monitoring intracellular H_2O_2 levels has a great significance[44]. Considering the excellent performance of HIL@Hb/MXene-Ti_3C_2/MGCE for H_2O_2 detection, we designed a 3D situ fixed cells electrode to detect H_2O_2 released from living 4T1 cells. Propylene glycol monomethyl ether acetate (PMA) was used as stimulating drugs. Fig. 5d shows the response current of 4T1 cells aroused by 20 μg mL^{-1} PMA. In contrast, no current response was observed in the control experiments either without PMA or with PMA-catalase (CAT) mixture, which confirms that the current responses were attributed to the drug induced H_2O_2 released from living cells. **Fig. S6** displays the current response collected from 3 chips, indicating that HIL@Hb/MXene--Ti_3C_2/MGCE chip can be used to actually measure H_2O_2 released by living cells.

3.5. Selectivity, reproducibility, and stability of biosensor

In order to better evaluate the feasibility and practical application of the HIL@Hb/MXene-Ti_3C_2/MGCE biosensor, we carried out selectivity, repeatability, and stability tests. To evaluate its selectivity, potentially interfering ions (0.5 mM of Glu, UA, AA, DA, NaCl, and KO_2) and H_2O_2 solution were added into 0.01 M PBS at pH of 7.24 and −0.35 V. In **Fig. S7**, the six interferents (3.98 μM) did not cause any current step, while a sharp current step was observed for H_2O_2 (3.98 μM), demonstrating that the HIL@Hb/MXene-Ti_3C_2/MGCE biosensor has excellent selectivity toward H_2O_2. To evaluate the stability of HIL@Hb/MXene-Ti_3C_2/MGCE, the biosensor was continuously used 30 times. As seen in Fig. 5e, the peak value of the CV curves did not exhibit any noticeable change, and 93% of the initial current response, was retained, which indicates that this sensing electrode has a good cycle stability. the Subsequently, the long-term stability of the biosensor was analyzed based on the current response after different storage times (Fig. 5f). The modified electrode was kept in a 4 °C refrigerator when not in use. Results showed that HIL@Hb/MXene-Ti_3C_2/MGCE retained about 90.11% of its primary current response to H_2O_2 after 30 days. The biocompatibility of HIL@Hb/MXene-Ti_3C_2 was further evaluated by live/dead double-staining assay using 4T1 cells. From **Fig. S8**, the 4T1 cells incubated with 0–100 μg/mL HIL@Hb samples exhibited negligible cell death, and those incubated with 200 μg/mL HIL@Hb showed only a small amount of cell death. This result indicates that HIL@Hb/Mxene-Ti_3C_2/MSPCE has good biocompatibility. All findings suggest that the designed HIL@Hb/MXene-Ti_3C_2/MGCE biosensor possesses excellent selectivity, good reproducibility, and long-time stability.

4. Conclusion

In this study, a method to prepare a hemoglobin-based biosensor is proposed, using $BBimPF_6$ as HIL and MXene-Ti_3C_2 nanosheets. Initially, an electrode was constructed with an HIL@Hb active layer and MXene-Ti_3C_2 modification layer, namely HIL@Hb/MXene-Ti_3C_2/MGCE. In which, the HIL@Hb active layer was formed via microfluidic control can effectively prevent aggregation and improve the stability and electrochemical activity of Hb, while MXene-Ti_3C_2 nanosheets can enhance the catalytic activity and stability of the biosensor. Compared with the electrode prepared with bulk HIL@Hb solution, HIL@Hb/MXene-Ti_3C_2/MGCE retained 93% activity after 30 uses and 90% activity after 30 days. In addition, we further found that the developed HIL@Hb/MXene-Ti_3C_2/MGCE biosensor has a good linear response range of 1.996–27.232 μM, detection limit reaching 1.996 nM (signal-to-noise ratio, $S/N = 3$), sensitivity of 52.08 $\mu A \cdot \mu M^{-1} \cdot cm^{-2}$. Which can detect hydrogen peroxide produced by cells in situ. This demonstrates that our proposed method can be effectively used to improve the stability of biosensors that have application significance in clinical diagnosis.

Credit author statement

Rongwei Gao: Major data contributions, Manuscript writing. **Yiqi Song:** Experimental aid. **Yuan Gao:** Biological data. **Xuelian Yang:** Experimental aid. **Shu-Juan Bao:** Supervision, Validation, Writing review & editing.

Declaration of competing interest

The authors declare that they have no known competing financial interests or personal relationships that could have appeared to influence the work reported in this paper.

Data availability

No data was used for the research described in the article.

Acknowledgements

We appreciate support from the National Natural Science Foundation of China (No. 21972111, 21773188), Fundamental Research Funds for the Central Universities(XDJK2019AA002, XDJK2019B052), Natural Science Foundation of Chongqing (cstc2018jcyjAX0714), Chongqing Engineering Research Center for Micro-Nano Biomedical Materials and Devices, Chongqing Key Laboratory for Advanced Materials and Technologies. Venture & Innovation Support Program for Chongqing Overseas Returnees (cx2019073). We also thank Yiqi Song, Yuan Gao, Xuelian Yang for help with this work.

Supplementary materials

Supplementary material associated with this article can be found, in the online version, at doi:10.1016/j.snr.2023.100146.

References

[1] Y.-H. Wang, C.-M. Yu, Z.-Q. Pan, Y.-F. Wang, J.-W. Guo, H.-Y. Gu, A gold electrode modified with hemoglobin and the chitosan@Fe_3O_4 nanocomposite particles for direct electrochemistry of hydrogen peroxide, Microchim. Acta 180 (2013) 659–667, https://doi.org/10.1007/s00604-013-0977-8.
[2] X.-M. Wang, Z.-J. Hu, P.-F. Guo, M.-L. Chen, J.-H. Wang, Purification of hemoglobin by adsorption on nitrogen-doped flower-like carbon superstructures, Microchim. Acta (2020) 187, https://doi.org/10.1007/s00604-020-4151-9.
[3] J. Gao, H. Liu, C. Tong, L. Pang, Y. Feng, M. Zuo, Z. Wei, J. Li, Hemoglobin-$Mn_3(PO_4)_2$ hybrid nanoflower with opulent electroactive centers for high-performance hydrogen peroxide electrochemical biosensor, Sensor. Actuat. B (2020) 307, https://doi.org/10.1016/j.snb.2019.127628.
[4] R. Gao, X. Yang, Q. Yang, Y. Wu, F. Wang, Q. Xia, S.J. Bao, Design of an amperometric glucose oxidase biosensor with added protective and adhesion layers, Microchim. Acta 188 (2021) 312, https://doi.org/10.1007/s00604-021-04977-w.
[5] Y. Sun, H. Du, Y. Lan, W. Wang, Y. Liang, C. Feng, M. Yang, Preparation of hemoglobin (Hb) imprinted polymer by Hb catalyzed eATRP and its application in biosensor, Biosens. Bioelectron. 77 (2016) 894–900, https://doi.org/10.1016/j.bios.2015.10.067.
[6] C.D. Spicer, E.T. Pashuck, M.M. Stevens, Achieving controlled biomolecule-biomaterial conjugation, Chem. Rev. 118 (2018) 7702–7743, https://doi.org/10.1021/acs.chemrev.8b00253.
[7] M. Lv, W. Zhou, H. Tavakoli, C. Bautista, J. Xia, Z. Wang, X. Li, Aptamer-functionalized metal-organic frameworks (MOFs) for biosensing, Biosens. Bioelectron. 176 (2021), 112947, https://doi.org/10.1016/j.bios.2020.112947.
[8] X. Lian, Y. Fang, E. Joseph, Q. Wang, J. Li, S. Banerjee, C. Lollar, X. Wang, H. C. Zhou, Enzyme-MOF (metal-organic framework) composites, Chem. Soc. Rev. 46 (2017) 3386–3401, https://doi.org/10.1039/c7cs00058h.
[9] C. Hu, Y. Bai, M. Hou, Y. Wang, L. Wang, X. Cao, C.-W. Chan, H. Sun, W. Li, J. Ge, K. Ren, Defect-induced activity enhancement of enzyme-encapsulated metal-organic frameworks revealed in microfluidic gradient mixing synthesis, Sci. Adv. 6 (2020) eaax5785, https://doi.org/10.1126/sciadv.aax5785.
[10] Q. Wang, G. Lu, B. Yang, Hydrogen peroxide biosensor based on direct electrochemistry of hemoglobin immobilized on carbon paste electrode by a silica sol–gel film, Sensor. Actuat. B 99 (2004) 50–57, https://doi.org/10.1016/j.snb.2003.10.008.
[11] C. Silva, M. Martins, S. Jing, J. Fu, A. Cavaco-Paulo, Practical insights on enzyme stabilization, Crit. Rev. Biotechnol. 38 (2018) 335–350, https://doi.org/10.1080/07388551.2017.1355294.
[12] N.R. Mohamad, N.H. Marzuki, N.A. Buang, F. Huyop, R.A. Wahab, An overview of technologies for immobilization of enzymes and surface analysis techniques for immobilized enzymes, Biotechnol. Biotech. Eq. 29 (2015) 205–220, https://doi.org/10.1080/13102818.2015.1008192.
[13] H. Liu, K. Guo, C. Duan, X. Dong, J. Gao, Hollow TiO_2 modified reduced graphene oxide microspheres encapsulating hemoglobin for a mediator-free biosensor, Biosens. Bioelectron. 87 (2017) 473–479, https://doi.org/10.1016/j.bios.2016.08.089.
[14] M. Eguilaz, R. Villalonga, G. Rivas, Electrochemical biointerfaces based on carbon nanotubes-mesoporous silica hybrid material: bioelectrocatalysis of hemoglobin and biosensing applications, Biosens. Bioelectron. 111 (2018) 144–151, https://doi.org/10.1016/j.bios.2018.04.004.
[15] Y. Wang, H. Zhang, Y. Kang, Z. Fei, J. Cao, The interaction of perfluorooctane sulfonate with hemoglobin: influence on protein stability, Chem. Biol. Interact. 254 (2016) 1–10, https://doi.org/10.1016/j.cbi.2016.05.019.
[16] I. Jha, P. Venkatesu, Unprecedented improvement in the stability of hemoglobin in the presence of promising green solvent 1-Allyl-3-methylimidazolium chloride, ACS Sustain. Chem. Eng. 4 (2015) 413–421, https://doi.org/10.1021/acssuschemeng.5b00939.
[17] Raja Jamaluddin, R.Z.A.;Yook Heng, L.L. L.;Tan, K.F. Chong, Electrochemical biosensor for nitrite based on polyacrylic-graphene composite film with covalently immobilized hemoglobin, Sensors (2018) 18, https://doi.org/10.3390/s18051343.

[18] J. Cui, Y. Zhao, R. Liu, C. Zhong, S. Jia, Surfactant-activated lipase hybrid nanoflowers with enhanced enzymatic performance, Sci. Rep. 6 (2016) 27928, https://doi.org/10.1038/srep27928.
[19] J. Cui, T. Lin, Y. Feng, Z. Tan, S. Jia, Preparation of spherical cross-linked lipase aggregates with improved activity, stability and reusability characteristic in water-in-ionic liquid microemulsion, J. Chem. Technol. Biot. 92 (2017) 1785–1793, https://doi.org/10.1002/jctb.5179.
[20] M. Baghayeri, H. Veisi, Fabrication of a facile electrochemical biosensor for hydrogen peroxide using efficient catalysis of hemoglobin on the porous Pd@Fe_3O_4-MWCNT nanocomposite, Biosens. Bioelectron. 74 (2015) 190–198, https://doi.org/10.1016/j.bios.2015.06.016.
[21] W. Yang, X. Zhou, N. Zheng, X. Li, Z. Yuan, Electrochemical biosensors utilizing the electron transfer of hemoglobin immobilized on cobalt-substituted ferrite nanoparticles–chitosan film, Electrochim. Acta 56 (2011) 6588–6592, https://doi.org/10.1016/j.electacta.2011.04.037.
[22] Z. Xuanliang, Z. Kanglin, Z. Yujia, L. Peng, L. Zechen, P. Jialiang, L. Yu, H. Meirong, B. Abdelrahman, Z. Hongwei, Hydrophobic ionic liquid-in-polymer composites for ultrafast, linear response and highly sensitive humidity sensing, Nano Res. (2020), https://doi.org/10.1007/s12274-020-3172-3.
[23] S. Xinjian, W. Bing, H. Yina, L. Liqing, L. Ting, L. Chunya, Z. Shenghui, A novel nanoporous film electrode based on electrochemical polymerization of ionic liquid and its application in sensitive determination of magnolol, Talanta (2014), https://doi.org/10.1016/j.talanta.2013.11.055.
[24] Q. Wang, M. Ge, X. Guo, Z. Li, A. Huang, F. Yang, R. Guo, Hydrophobic poly(ionic liquid)s as “two-handed weapons”: maximizing lipase catalytic efficiency in transesterification of soybean oil toward biodiesel, Appl. Catal. A (2021) 626, https://doi.org/10.1016/j.apcata.2021.118350.
[25] Y. Shu, D. Cheng, X. Chen, J. Wang, A reverse microemulsion of water/AOT/1-butyl-3-methylimidazolium hexafluorophosphate for selective extraction of hemoglobin, Sep. Purif. Technol. 64 (2008) 154–159, https://doi.org/10.1016/j.seppur.2008.09.010.
[26] D.H. Cheng, X.W. Chen, Y. Shu, J.H. Wang, Selective extraction/isolation of hemoglobin with ionic liquid 1-butyl-3-trimethylsilylimidazolium hexafluorophosphate (BtmsimPF_6), Talanta 75 (2008) 1270–1278, https://doi.org/10.1016/j.talanta.2008.01.044.
[27] M.S. Lopez, D. Mecerreyes, E. Lopez-Cabarcos, B. Lopez-Ruiz, Amperometric glucose biosensor based on polymerized ionic liquid microparticles, Biosens. Bioelectron. 21 (2006) 2320–2328, https://doi.org/10.1016/j.bios.2006.02.019.
[28] T. Priemel, G. Palia, F. Forste, F. Jehle, S. Sviben, I. Mantouvalou, P. Zaslansky, L. Bertinetti, M.J. Harrington, Microfluidic-like fabrication of metal ion-cured bioadhesives by mussels, Science 374 (2021) 206, https://doi.org/10.1126/science.abi9702. -+.
[29] M. Krogsgaard, M.R. Hansen, H. Birkedal, Metals & polymers in the mix: fine-tuning the mechanical properties & color of self-healing mussel-inspired hydrogels, J. Mater. Chem. B 2 (2014) 8292–8297, https://doi.org/10.1039/c4tb01503g.
[30] E. Khare, N. Holten-Andersen, M.J. Buehler, Transition-metal coordinate bonds for bioinspired macromolecules with tunable mechanical properties, Nat. Rev. Mater. 6 (2021) 421–436, https://doi.org/10.1038/s41578-020-00270-z.
[31] S.F. Zhao, F.X. Hu, Z.Z. Shi, J.J. Fu, Y. Chen, F.Y. Dai, C.X. Guo, C.M. Li, 2-D/2-D heterostructured biomimetic enzyme by interfacial assembling Mn-$_3(PO_4)_{(2)}$ and MXene as a flexible platform for realtime sensitive sensing cell superoxide, Nano Res. 14 (2021) 879–886, https://doi.org/10.1007/s12274-020-3130-0.
[32] L. Xin, L. Yanli, L. Qingjun, Electrochemical and optical biosensors based on multifunctional MXene nanoplatforms: progress and prospects, Talanta (2021), https://doi.org/10.1016/j.talanta.2021.122726.
[33] S. Neampet, N. Ruecha, J. Qin, W. Wonsawat, O. Chailapakul, N. Rodthongkum, A nanocomposite prepared from platinum particles, polyaniline and a Ti_3C_2 MXene for amperometric sensing of hydrogen peroxide and lactate, Microchim. Acta (2019) 186, https://doi.org/10.1007/s00604-019-3845-3.
[34] L. Lorencova, T. Bertok, E. Dosekova, A. Holazova, D. Paprckova, A. Vikartovska, V. Sasinkova, J. Filip, P. Kasak, M. Jerigova, D. Velic, K.A. Mahmoud, J. Tkac, Electrochemical performance of Ti_3C_2Tx MXene in aqueous media: towards ultrasensitive H_2O_2 sensing, Electrochim. Acta 235 (2017) 471–479, https://doi.org/10.1016/j.electacta.2017.03.073.
[35] Q. Yang, T. Yang, W. Gao, Y. Qi, B. Guo, W. Zhong, J. Jiang, M. Xu, An MXene-based aerogel with cobalt nanoparticles as an efficient sulfur host for room-temperature Na–S batteries, Inorg. Chem. Front. 7 (2020) 4396–4403, https://doi.org/10.1039/D0QI00939C.
[36] X. Yang, W. Qiu, R. Gao, Y. Wang, Y. Bai, Z. Xu, S.-J. Bao, MIL-47(V) catalytic conversion of H_2O_2 for sensitive H_2O_2 detection and tumor cell inhibition, Sensor. Actuat. B (2022) 354, https://doi.org/10.1016/j.snb.2021.131201.
[37] K. Agrawal, P. Verma, Laccase: addressing the ambivalence associated with the calculation of enzyme activity, 3 Biotech 9 (2019) 365, https://doi.org/10.1007/s13205-019-1895-1.
[38] K.S. Egorova, E.G. Gordeev, V.P. Ananikov, Biological activity of ionic liquids and their application in pharmaceutics and medicine, Chem. Rev. 117 (2017) 7132–7189, https://doi.org/10.1021/acs.chemrev.6b00562.
[39] M. Masuda, Y. Motoyama, J. Kuwahara, N. Nakamura, H. Ohno, A paradoxical method for NAD+/NADH accumulation on an electrode surface using a hydrophobic ionic liquid, Biosens. Bioelectron. 39 (2013) 334–337, https://doi.org/10.1016/j.bios.2012.07.051.
[40] K. Ren, Y. Chen, H. Wu, New materials for microfluidics in biology, Curr. Opin. Biotechnol. 25 (2014) 78–85, https://doi.org/10.1016/j.copbio.2013.09.004.
[41] S. Dong, P. Zhang, H. Liu, N. Li, T. Huang, Direct electrochemistry and electrocatalysis of hemoglobin in composite film based on ionic liquid and NiO microspheres with different morphologies, Biosens. Bioelectron. 26 (2011) 4082–4087, https://doi.org/10.1016/j.bios.2011.03.039.
[42] S.-J. Bao, C.M. Li, J.-F. Zang, X.-Q. Cui, Y. Qiao, J. Guo, New nanostructured TiO_2 for direct electrochemistry and glucose sensor applications, Adv. Funct. Mater. 18 (2008) 591–599, https://doi.org/10.1002/adfm.200700728.
[43] T. Liang, L. Zou, X. Guo, X. Ma, C. Zhang, Z. Zou, Y. Zhang, F. Hu, Z. Lu, K. Tang, C. M. Li, Rising mesopores to realize direct electrochemistry of glucose oxidase toward highly sensitive detection of glucose, Adv. Funct. Mater. (2019) 29, https://doi.org/10.1002/adfm.201903026.
[44] S. Cui, L. Li, Y. Ding, J. Zhang, Q. Wu, Z. Hu, Uniform ordered mesoporous $ZnCo_2O_4$ nanospheres for super-sensitive enzyme-free H_2O_2 biosensing and glucose biofuel cell applications, Nano Res. 10 (2017) 2482–2494, https://doi.org/10.1007/s12274-017-1452-3.